J. theor. Biol. (2002) **216,** 367–385
doi:10.1006/jtbi.2001.2504, available online at http://www.idealibrary.com on IDEAL®

A Method for the Calculation of Odor Character from Molecular Structure

L. TURIN*

Department of Physiology, University College London, Gower St, London WC1E6BT, UK

(*Received on* 30 *August* 2001, *Accepted in revised form on* 22 *November* 2001)

The relationship between molecular structure and odor character is one of the most complex structure–activity problems in biology. Despite over a century of effort, it remains unsolved, and synthesis of new odorants still proceeds largely by trial and error. In previous work, I have argued that the reason for this failure lies in a mistaken assumption, namely that molecular shape determines odor character. Instead, I have taken up and extended an old idea (Dyson, 1938) according to which vertebrate olfactory receptors detect odorants by their molecular vibrations. I propose that the detection mechanism is inelastic electron tunnelling. If this is correct, there should be a correlation between the tunnelling vibrational spectra of odorants and their odor character. Here, using semi-empirical quantum chemistry methods and a simple calculation method for tunnelling mode intensities, I calculate the spectra of structurally diverse odorants belonging to various odor categories. With few exceptions, the calculated spectra of bitter almonds, musks, ambers, woods, sandalwoods and violets strongly correlate with odor character.

1. Introduction

Attempts at correlating molecular structure with odor character are as old as synthetic chemistry itself (for a historical review see Moncrieff, 1949). Inspired by the success of "lock and key" theories in other areas of biology, most start with the assumption that molecular shape determines odor. However, despite an odorant database of hundreds of thousands of molecules, no clear relationship between shape and odor has emerged. Indeed, a recent review candidly concludes that shape-based structure–odor relations are in a "sorry state" (Fráter *et al.*, 1998). A practical consequence is that synthetic efforts among the handful of companies involved in making new odorants still proceed by trial and error.

*E-mail: l.turin@ucl.ac.uk

Ultimately, odor is a biological problem (Sell, 1999) and a successful theory must take into account our rapidly increasing understanding of olfactory receptors. Two theories currently purport to explain the "reading" of molecular structure by olfactory receptors, the odotope theory and the vibration theory. The pros and cons of these two theories have been recently reviewed by Turin & Yoshii (2002), and only a sketchy description of their features will be given here.

According to adotope theory (Mori & Shepherd, 1994), different receptors bind to structural motifs of the odorant, and the pattern of receptor activation is interpreted by the brain to identify in a unique fashion the whole odorant molecule. The main evidence for this theory is that identified receptor subtypes respond not to one, but to many odorants (see for example Malnic *et al.*, 1999). Assuming

0022-5193/02/$35.00/0

their recognition to be based on shape, this suggests that the receptors are binding to a feature shared by the odorants, or odotope. The number and nature of odotopes is not known, and for the moment odotope theory has little predictive power.

Vibration theory is an old idea, first proposed by Dyson (1938), and later expanded by Wright (1977). It states that odor character is determined by the vibrational spectrum of the molecule. Turin (1996) provided a mechanism for detection of vibrations by suggesting that receptors were a biological embodiment of an inelastic electron tunnelling spectroscope (IETS). The reader is referred to Turin (1996) and Turin and Yoshii (2002) for a detailed account of the evidence supporting this theory. For the purposes of this article, it is sufficient to recall that (a) vibrational mode energies (frequencies) are supposed to be those of the molecule in solution (b) the sensing mechanism is postulated to be electron scattering and therefore mode intensities differ from those observed by IR and Raman methods and (c) the sensing is done in N receptor "bands" resembling those of color vision pigments [see Fig. 16(a)].

The vibrational spectrum (0–4000 cm^{-1}) is made up of two halves. Above 1700 cm^{-1}, vibrational modes are mostly due to stretching of atom pairs, as in C=O, C≡N, S–H, C–H, N–H and O–H. Below 1700 cm^{-1}, most of the modes are complex involving three or more atoms. Vibrational theory explains our ability to recognize the presence of odorant functional group stretch modes in the upper half of the spectrum, e.g. the fact that we unerringly distinguish SH and OH groups in odorants. By contrast, the lower half will determine odor character of different odorants bearing the same functional group, and is the subject of this paper. Vibrational theory can readily be tested in principle. If the vibrational energies and intensities could be calculated exactly, the spectra of molecules as perceived by our noses could be determined and compared. If in addition, the number, position and width of the N sensing bands were known, odor character could be computed exactly as a point in N-dimensional space. Neither is possible at this point. However, it is possible to compute approximate spectra using a simplified version of IETS theory, and blurred by the estimated sensors' energy resolution (Turin, 1996). Calculating these spectra for even a small fraction of known odorants is a huge task, and may be pointless until the algorithm is properly benchmarked. Instead, this paper illustrates its strengths and limitations in a few selected cases.

2. Method

2.1. VIBRATIONAL MODES

Advances in computing power and in software interfaces now make it both quick and easy to calculate the vibrational modes of molecules using a variety of semiempirical and, more recently, *ab initio* quantum chemistry software packages. The one chiefly used in the calculations described below was MacSpartan Pro (Wavefunction Inc, Irvine, CA). Typically, the time taken by quantum chemistry computations scales as a high power of the number of electrons in the molecule. Fortunately, all odorants are below 300 Da in molecular weight, and all but a few are made up of the elements C, H, O, N, and S. This translates in computing times from structural input into optimization and mode calculation ranging from minutes on a moderately fast PC (iMac G3 333 MHz) for semiempirical methods, to days for *ab initio* methods.

The computation of vibrational mode energies is itself subject to a number of choices and assumptions. First, different parameter sets exist that describe the orbitals used to build up computational models of molecules. Semiempirical methods calculate modes with a margin of error of a few tens of wavenumbers (cm^{-1}, 1 cm^{-1} ≈0.123 meV). The vibrational range for odorants is typically from 50 to 3400 cm^{-1}. Turin (1996) has argued that the range below 5–600 cm^{-1} is unlikely to be sensed. Thus in the 500–3400 range an error of, say, 30 cm^{-1} is a 0.8–6% error, which is probably tolerable, given the resolution of the system (see Section 5). This margin of error only applies to representations of the most common elements (C, H, O and N). Even with S, semiempirical methods can make large errors. For example SH stretch (2500–2600 cm^{-1} experimentally) is calculated to be

2037, 1808 and 2988 (uncorrected) by semiempirical methods using AM1, PM3 and MNDO parameter sets, respectively. *Ab initio* methods perform much better, predicting 2947, 2614 and 2628 cm^{-1} (corrected with $F = 0.9$) for STO 3G, 3-21G(*) and 6-31G* basis sets, respectively. Clearly, computations of odorants containing even mildly exotic heteroatoms must be done with care. Fortunately, these are in a small minority. One exception is the class of molecules possessing the camphoraceous character, where *ab initio* methods would be needed to treat accurately such odorants as hexachloroethane, triethylamine-borane and thiophosphoric acid dichloride ethyl amide (Rossiter, 1996).

2.2. PARTIAL CHARGES ON ATOMS

Inelastic electron tunnelling spectroscopy (IETS) involves the scattering of electrons by molecular charges. Even when, as is the case for all odorants, a molecule has no overall charge, the electron density is not everywhere appropriate to exact cancellation of nuclear charge, and regions of negative (electron-rich) and positive (electron-deficient) charge exist. These can be interpreted as partial charges on individual atoms. Partial charges are not experimental observables, but can be inferred from dipole intensities in the IR, etc. In the calculations described below, the MNDO parameter set was chosen for semiempirical calculation because it estimates most accurately the partial charges crucial to IETS scattering (Hehre *et al*., 1998). In Turin (1996) Mulliken charges were used. In addition, electrostatic partial charge calculation method has been used. It derives from the overall charge density a distribution of point charges situated at the position of constituent atom nuclei that would give the observed electric field.

2.3. SENSOR BANDS: NUMBER, POSITION AND WIDTH

This is perhaps the most difficult set of parameters to estimate. Turin (1996) assumed that sensor bands would be 400 cm^{-1} wide, and therefore that ten at most would be needed to "tile" the vibrational spectrum. The width of the sensor bands ultimately depends on how narrow the distribution of electron energies in the receptor is. This width is not known and is hard to guess at, but 400 cm^{-1}, or 1.5 kT is plausible. In the plots described in Section 5, four bands centred on 500, 100, 1300 and 1500 cm^{-1} were used. This is because (a) this enables after normalization a convenient three-dimensional representation of the data and (b) that number was found to be sufficient to discriminate the odorants, in this study.

2.4. THE ALGORITHM

The calculation of mode intensities proceeds according to a much-simplified version of the method of Sleigh *et al*. (1986). For each vibrational mode, and for each atom i : 1...N of the N-atom molecule, the displacements x_i (usually given as Cartesian displacements in x, y and z) and partial charges q_i are calculated by the chemistry software. The results are made available as a text file. From this q_i's and x_i's are extracted and the mode intensity

$$\sum_{i=1}^{N} q_i^2 x_i^2$$

is calculated for each mode. In the present paper, the extraction of the relevant number from the text file and subsequent computation was done using LabView software (National Instruments). This yields the raw spectrum, with each mode represented by a pair of numbers, namely energy (wavenumbers, abscissa), and intensity ($e^2Å^2$, ordinate). The spectrum is then convolved with a Gaussian function of width (2 S.D.) 100 cm^{-1}.

2.5. AN EXAMPLE SPECTRUM: *TRANS*-2-HEXENAL

Figure 1 shows the unconvolved and convolved spectra of *trans*-2-hexenal. The vertical lines are individual vibrational modes, the curve the spectrum convolved with the blurring Gaussian. The types of modes responsible for the peaks are indicated above the curve. Note that all wavenumbers are uncorrected and therefore higher than their experimental values: for example C = O stretch is at 2114 cm^{-1} rather than $\approx$1800 cm^{-1}, etc. To provide the reader with data for comparison with other software packages that may use slightly different MNDO parameter sets, the partial charges and

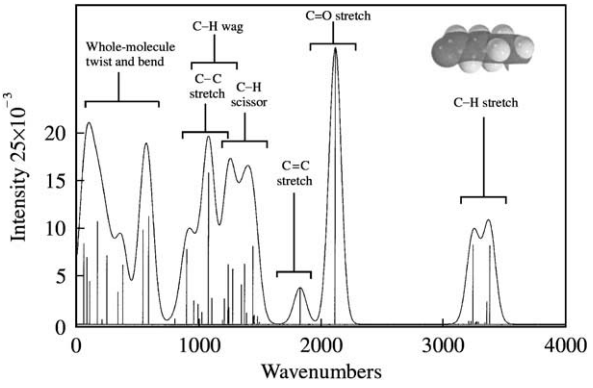

FIG. 1. The spectrum of *trans*-2-hexenal (inset). The calculated peaks are shown before (vertical bars) and after (smooth curve) convolution with a Gaussian (S.D. = 100 wavenumbers). Types of vibrations responsible for different sections of the spectrum are indicated.

vibrational modes of a small molecule (*trans*-2-hexenal) are given in Appendix A.

3. Results

3.1. CHOICE OF ODORANT DATA SET

Most previous attempts at structure–odor relation (SOR) theories were local, that is to say restricted to a set of related molecules possessing a given odor character. Perhaps because of this, there is no commonly agreed reference data set of odorants on which to test a *general* SOR theory. When constructing such a set from published odor character data, a great deal has to be taken on faith. Odor character can be distorted by traces of contaminants, and the description is frequently influenced by extraneous factors. For example, the term "floral" is often used to describe odorants which can be used in floral formulations but do not in themselves smell floral at all, e.g. indole. Furthermore, many molecules of interest to SOR studies are not commercially available, and frequently difficult to obtain from the chemists who described their structure and odor in the literature. I have found that the most reliable odor profiles come, not surprisingly, from studies performed by fragrance firms, where they are assessed by professional perfumers or where the chemists themselves have perfumery experience. Most of the profiles in this study come from Arctander (1994), Boelens (1974), Fráter *et al.* (1999) Moncrieff (1949), Ohloff (1994), Rossiter (1996) and Sell (1999). This study deals only with the broadest odor categories such as musk, amber, wood, sandalwood and violets, about which there is little disagreement. The odorants described in this study are shown in Fig. 2.

3.2. STRUCTURE SENSITIVE AND STRUCTURE-INSENSITIVE MAPS

Arguably, the most puzzling feature of structure–odor relations, which has frustrated attempts at systematization, is the fact that very small changes in structure can lead to large changes in odor (structure-sensitive), but just as often very large ones do not (structure-insensitive). What this means is that the mapping from structure to odor is folded in a complex and so far unpredictable manner. A successful odor calculation algorithm should predict this correctly.

3.2.1. *Structure Sensitive*

Caution is required when choosing published examples of big odor change caused by a small structural change, because the alteration most frequently described is not a change in odor character proper, but one from odorant to "odorless". As Turin and Yoshii (2001) point out, "odorless" frequently means "orders of magnitude less powerful than the reference compound", and begs the question of what the remaining, weak odor character might be. Further, we have argued that, in a vibrational theory, odorless *cannot* be an odor character because all molecules have a vibrational spectrum. It must therefore be entirely determined by affinity of the molecule for its receptor(s), In other words, odorless molecules are not sensed at all, rather than sensed and found to be odorless. Only changes in odor character proper will be considered in this section. Odor intensity is *not* predicted by this algorithm.

FIG. 2. Structures of the odorants described in this study. Molecules are arranged by categories: SS: structure sensitive. B: bitter almonds S: structure insensitive M: musks A: ambers W: woods and SW: sandalwoods. The structures are taken from Arctander (1994) Boelens (1974), Rossiter (1996) and Fràter *et al.* (1999).

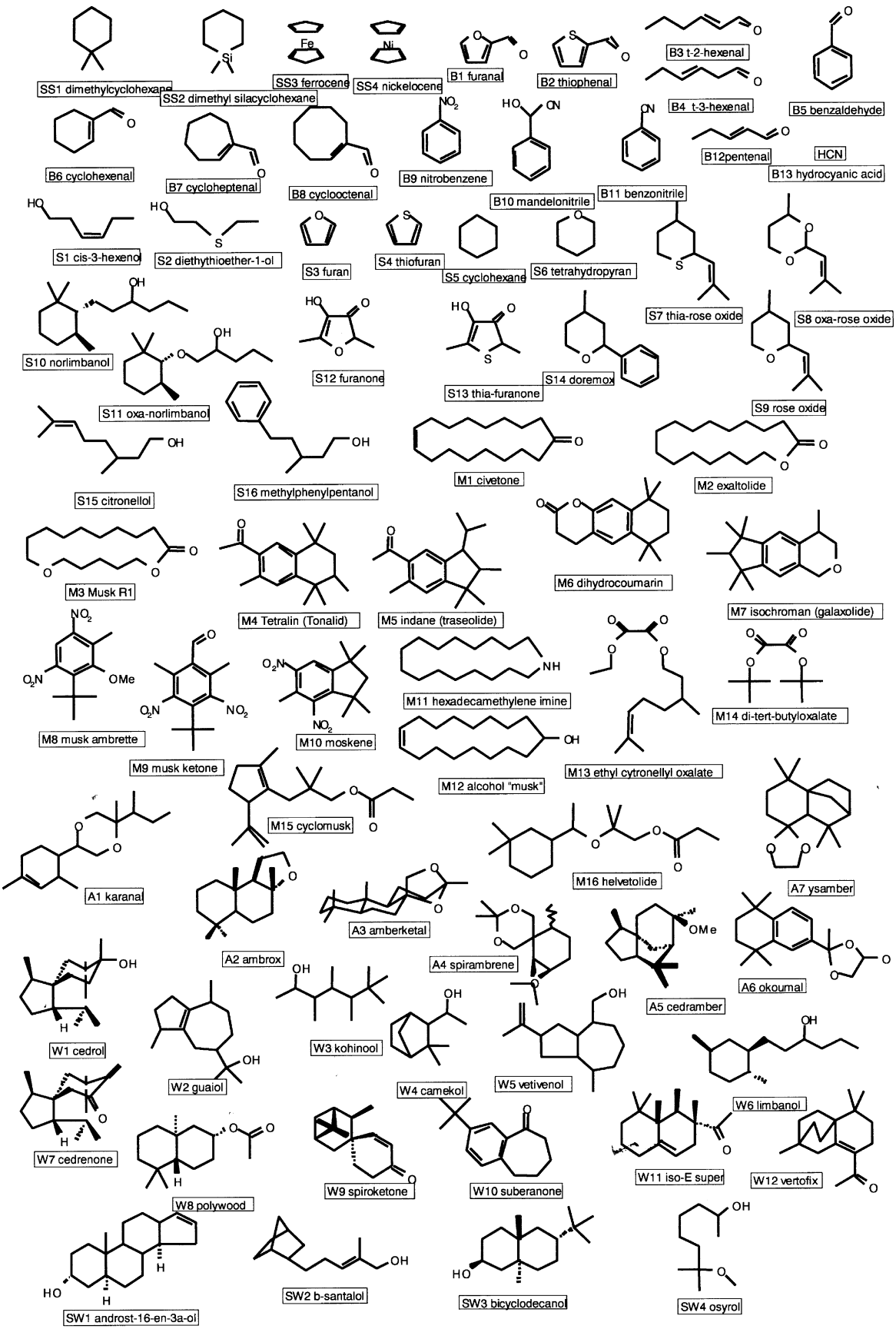
SS1 dimethylcyclohexane
SS2 dimethyl silacyclohexane
SS3 ferrocene
SS4 nickelocene
B1 furanal
B2 thiophenal
B3 t-2-hexenal
B4 t-3-hexenal
B5 benzaldehyde
B6 cyclohexenal
B7 cycloheptenal
B8 cyclooctenal
B9 nitrobenzene
B10 mandelonitrile
B11 benzonitrile
B12pentenal
HCN
B13 hydrocyanic acid
S1 cis-3-hexenol
S2 diethythioether-1-ol
S3 furan
S4 thiofuran
S5 cyclohexane
S6 tetrahydropyran
S7 thia-rose oxide
S8 oxa-rose oxide
S9 rose oxide
S10 norlimbanol
S11 oxa-norlimbanol
S12 furanone
S13 thia-furanone
S14 doremox
S15 citronellol
S16 methylphenylpentanol
M1 civetone
M2 exaltolide
M3 Musk R1
M4 Tetralin (Tonalid)
M5 indane (traseolide)
M6 dihydrocoumarin
M7 isochroman (galaxolide)
M8 musk ambrette
M9 musk ketone
M10 moskene
M11 hexadecamethylene imine
M12 alcohol "musk"
M13 ethyl cytronellyl oxalate
M14 di-tert-butyloxalate
M15 cyclomusk
M16 helvetolide
A1 karanal
A2 ambrox
A3 amberketal
A4 spirambrene
A5 cedramber
A6 okoumal
A7 ysamber
W1 cedrol
W2 guaiol
W3 kohinool
W4 camekol
W5 vetivenol
W6 limbanol
W7 cedrenone
W8 polywood
W9 spiroketone
W10 suberanone
W11 iso-E super
W12 vertofix
SW1 androst-16-en-3a-ol
SW2 b-santalol
SW3 bicyclodecanol
SW4 osyrol

3.2.2. *Sila Compounds*

Turin and Yoshii have discussed the significance of odorants in which a carbon atom is replaced with its group neighbor in the periodic table, silicon (Wannagat *et al.*, 1993). This preserves bond angles, increases bond lengths slightly and modifies partial charges, because the Si–C bond is more polar than is C–C congener. Fig. 3(a) illustrates the structures and computed spectra of the commercially available (Lancaster Synthesis) dimethylcyclohexane and dimethyl*sila*cyclohexane. The *sila* replacement amounts to a relatively small structural change, accompanied by a striking change in odor character, from camphoraceous to harsh, bleach-like. Unsurprisingly, given the different mass and partial charge of the silicon atom, the spectra are very different. Similar results are found with all *sila* replacements.

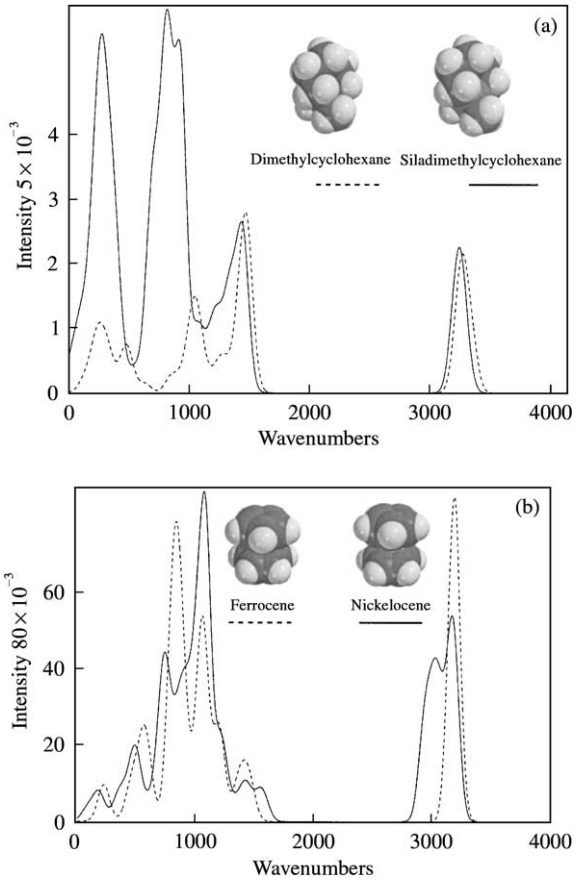

FIG. 3. Structures and spectra of (a) 1,1 dimethylcyclohexane and 1,1 dimethylsilacyclohexane and (b) two metallocenes, ferrocene and nickelocene. Despite the small change in structure, spectra (and odor character) are markedly different in both instances.

3.2.3. *Metallocenes*

As was pointed out in Turin (1996) and Turin & Yoshii (2002) metallocences provide a useful instance of minimal structural change accompanied by a large change in odor. Ferrocene smells camphoraceous, whereas nickelocene, in which the central divalent iron ion is replaced by a nickel ion, has an unpleasant, sweetish smell reminiscent of cycloheptatriene. The spectra are shown below in Fig. 3(b). Note that in this instance, semiemprirical calculations were performed using PM3 parameters, because the MNDO set of MacSpartan Pro does not include Fe and Zn. The spectra are very different.

3.3. STRUCTURE INSENSITIVE

3.3.1. *Bitter Almonds*

Bitter almonds always have pride of place in any SOR review, because they represent an extreme case of structural convergence. The bitter almond character has been reported in upwards of 70 molecules, all <150 Da. What is unique about the bitter almonds category is that a very small, linear molecule, HCN, also possesses the odor character. Structural rules have been empirically determined for bitter almond odorants other than HCN, but HCN does not fit them. To account for this, Sell (1999) has argued the interesting notion that since HCN and benzaldehyde are decomposition products of mandelonitrile present in bitter almonds, they have become associated, and the same odor has been "given" to both by the brain.

For a vibrational theory, the bitter almonds case is particularly valuable, because HCN only has three vibrational modes: a bending mode at 792 cm^{-1}, CN stretch at 2094 cm^{-1} and CH stretch at 3213 cm^{-1}. Based on data calculated by an earlier version of this algorithm, Turin (1996) argued that bitter almonds was a "bichromatic" odor, and that organic (non HCN) bitter almond odorants all had prominant modes at the correct frequencies. Figure 4(a) shows the recalculated spectra for eight classic bitter almond odorants together with the convolved peaks for HCN (experimental wavenumber values, arbitrary amplitudes). The most prominent

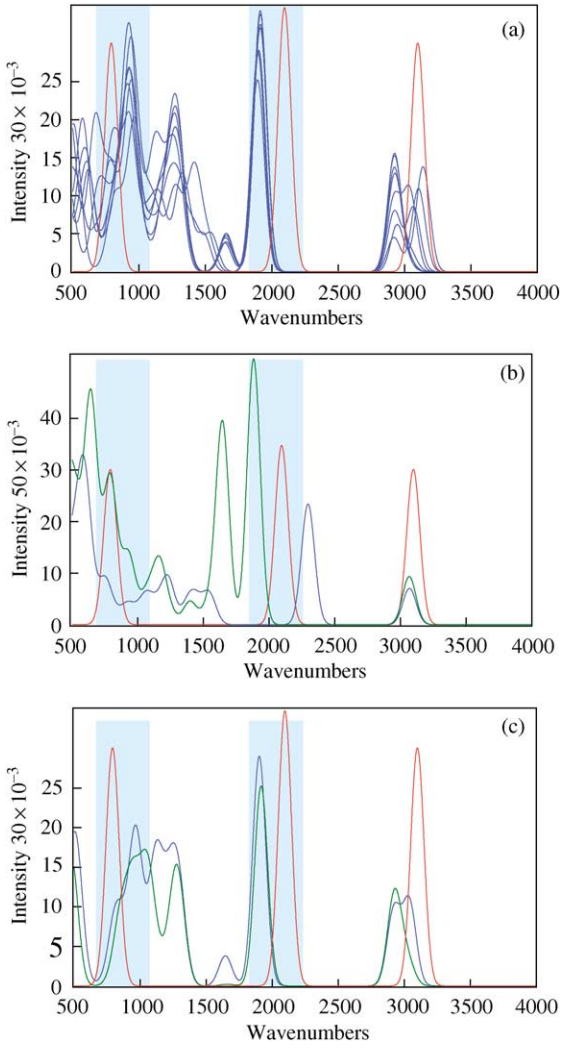

FIG. 4. (a) The spectra of eight bitter almond odorants, A1–A8 in Fig. 1 in blue, superimposed on the three peaks of HCN (experimental values, amplitudes arbitrary). All the bitter almond odorants have two peaks in postulated bands responsible for bitter almonds odor. To allow comparison with experimental values of HCN, calculated wavenumber values have been scaled by 0.9. (b) the spectra of nitrobenzene (green) and benzonitrile (blue). Nitrobenzene fits the HCN pattern (red) but benzonitrile does not. (c) The spectra of a "borderline" bitter almonds odorant (*trans*-2-hexenal) and its "green" isomer *trans*-3-hexenal. The peak at 1000 wavenumbers is smaller the green isomer.

doi: 10:1006 jtbi.2001.2504

peak for all these odorants in the region below $1500\,cm^{-1}$ lies near $920\,cm^{-1}$ and matches reasonably well the HCN bend frequency. The "920" cm^{-1} peak is in all cases due to one or two intense modes. The aromatic bitter almond odorants all have one or two intense (in-plane and out-of-plane) ring breathing modes coupled to aldehyde motion. The aliphatic ones have an out-of-plane CH wag involving the aldehyde and the carbons on either side of the double bond. Remarkably, these bending modes all involve the "odotope" (C = C–C = O) identifies by Zakarya *et al*. (1993) as responsible for the odor of bitter almonds. Nitrobenzene (Fig. 4(b)] also gives a good fit to the HCN "bands". By contrast, benzonitrile [Fig. 4(b)] does not fit the pattern and shows no particular peak in the $900\,cm^{-1}$ band. This is hard to interpret. It could be due to a miscalculation of the partial charges and/or mode energies. It may also be due to a misclassification: benzonitrile, to this author's nose at least, has only the weakest trace of bitter almonds character and a strong oily-metallic nitrile character. The bitter almonds note could be due to an HCN impurity.

Figure 4(c) illustrates a "borderline" bitter almond odorant, *trans*-2-hexenal, which smells green (e.g. cut grass) to some observers and bitter almonds to others (the author among them). What makes it interesting is that the isomer *trans*-3-hexenal has no bitter almond character, thereby allowing a direct comparison. The peak around $1000\,cm^{-1}$ in the *trans*-2-hexenal (though smaller than in other organic bitter almonds) is absent in *trans*-3-hexenal.

3.3.2. *Cis-3-hexenol and its Sulfur Congener*

Replacement of the C = C double with a–S-atom in *cis*-3 hexenol leads to a marked change in structure with remarkably little change in odor character (Boelens & Heydel, 1973). The computed spectra for these two molecules (Fig. 5) are remarkably similar. This is not because the underlying unconvolved peaks are identical. The inset shows the peak around 1500 wavenumbers at higher magnification, together with the unconvolved peaks shown as a bar graph. The peak around $1500\,cm^{-1}$, for example, which in the *cis*-3-hexenol is due a single complex CH_2 wag mode, is replaced by three separate modes of lower intensity in the –S–compound. When convolved, these add up to approximately the same overall intensity.

3.3.3. *Replacement of C with O, O with S without Odor Character Changes*

There are a few unusual examples of molecules in which these replacements do not markedly affect odor, as described by Ohloff (1994). The replacement of O with S in rose oxide [Fig. 6(a)] reportedly has a small effect on character; replacing a carbon with an oxygen atom in the rose oxide ring [Fig. 6(b)] leaves the smell unaltered, as do replacing a carbon with an oxygen in the side- chain of norlimbanol [Fig. 6(c)], and O by S in a furanone derivative [Fig. 6(d)]. The computed spectra reflect this.

Replacement of C with O, and of O with S in general profoundly affects odor character, as witnessed for example by the difference in smell between furan (spicy smokey) and thiofuran (benzenic) [spectrum in Fig. 7(a)], and between cyclohexane ("solvent" odor) and tetrahydropyran (pungent-sweetish) (not shown). The computed spectra for these molecules are quite different from each other.

3.3.4. *The Isobutenyl–Phenyl Replacement*

A remarkable and well-documented instance of structural change accompanied by small changes in odor character is the replacement of an isobutenyl group with a phenyl group (Sturm, 1978). This is usually attributed to the similarity in shape between isobutenyl and phenyl (see for example Kraft *et al*., 1999). Indeed, if one neglects the large difference in extent and geometry of π orbitals, the two groups have similar volume, and surface area. The idea that their interchangeability in odorants is due to their similarity in shape is, however, inconsistent with the fact that benzene and isobutene have very different odors, respectively, aromatic and gassy. There are many documented instances of the isobutenyl–phenyl replacement. I have chosen two described in Boelens (1974) and Frater *et al*. (1998): those of citronellol and rose oxide

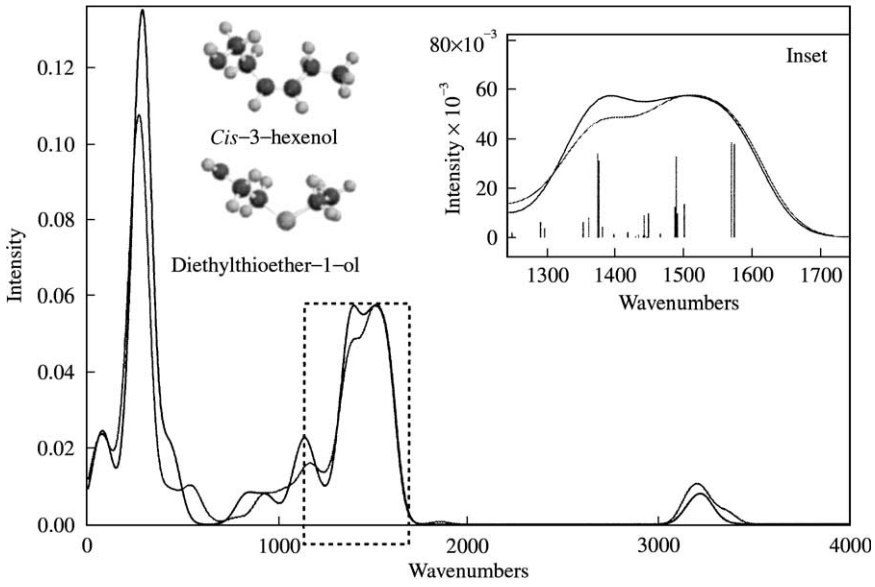

FIG. 5. Structures and spectra of *cis*-3-hexenol and diethylthioether-1-ol. Despite a considerable change in structure, the spectra are remarkably similar. The inset shows the unconvolved peaks underlying the region between 1300 and 1600 wavenumbers where the convolved spectra follow each other closely. Note that a different distribution of unconvolved modes is involved in the two odorants.

(normally isobutenyl). Isobutenyl–phenyl replacement in citronellol and rose oxide causes little change in odor. The algorithm predicts this correctly. The graphs are very close indeed to each other [Fig. 7(c and d)]. Note that this is not a straightforward "sum of the parts" effect. When the isobutenyl and phenyl groups are calculated separately, each with an atom added to represent the rest of the molecule, and this atom is held fixed in the calculations, two completely different spectra are obtained [Fig. 7(b)]. The results of Fig. 7(c and d) are clearly due to interactions of the two groups with the rest of the molecule affecting vibrational modes that are not, of course, confined to one or the other part.

In summary, these results suggest that the algorithm correctly predicts the "distance" in odor space of odorants in which a structural change causes either a large or a small odor change.

4. Prediction of Odor Categories

4.1. MUSKS

Musks are commercially important, and therefore have generated a lot of synthetic interest from the 1880's to the present. Thousands of musk compounds have been described in the literature. Commercially available musks fall into four structurally very different classes: polycyclics (indanes, isochromans and tetralins); nitros derived from the first synthetic musk discovered by Baur in 1888; macrocyclics derived from natural musks; and some recently discovered ester musks (helvetolide and cyclomusk) (see Kraft *et al.*, 2000 for a review). Though they smell different from one another, they nevertheless have a strong resemblance, in the sweet, powdery, clean character known as musky. Calculated spectra for three macrocyclic, three polycyclic and two ester musks are shown in Fig. 8(a), and for three nitro musks in Fig. 8(b). These clearly show that despite large structural differences, certain spectral features are common to musks in the three structural classes. They are: three prominent bands around 700, 1500 (1750 for the nitros) and 2200 cm^{-1} (carbonyl stretch). In between the first and the second band, there is another weak band around 1000 cm^{-1}. Fig. 8(a and b) illustrates how these might be sensed by three receptor bands situated at 700, 1600 and 2100 cm^{-1} to give a very similar excitation pattern. Note, however, that the algorithm fails to predict the smell of the isochroman musk galaxolide in whose spectrum the prominent 700 cm^{-1} band is absent [Fig. 8(c)].

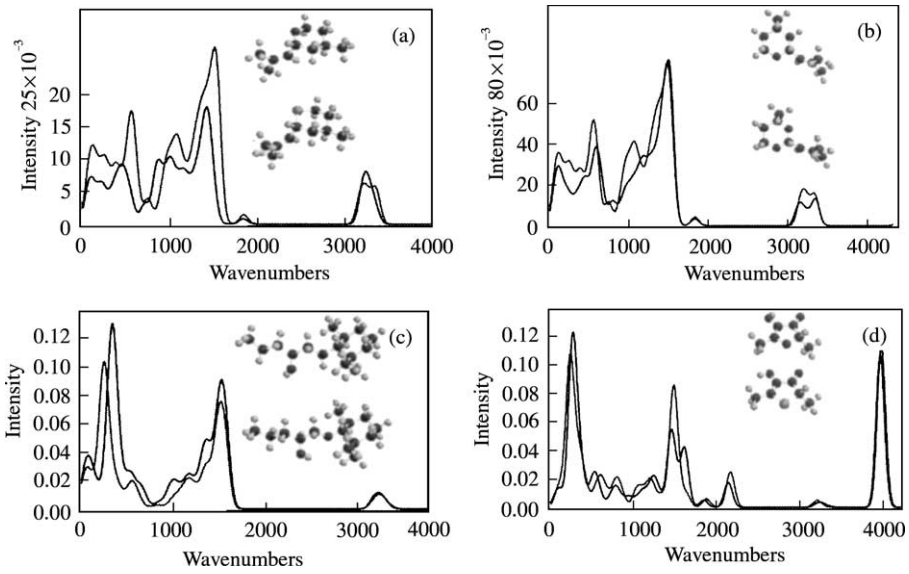

FIG. 6. Spectra of four pairs of odorants where, unusually, replacement of one element for another does not markedly change the odor character. (a) rose oxide and thia congener (b) rose oxide and oxa congener 4-methyl-2-(2-methyl-1-propenyl)1,3 dioxane (c) norlimbanol and oxa congener (d) furanone and thia congener. In all cases, the (unscaled) spectra are quite similar, as are the odor characters.

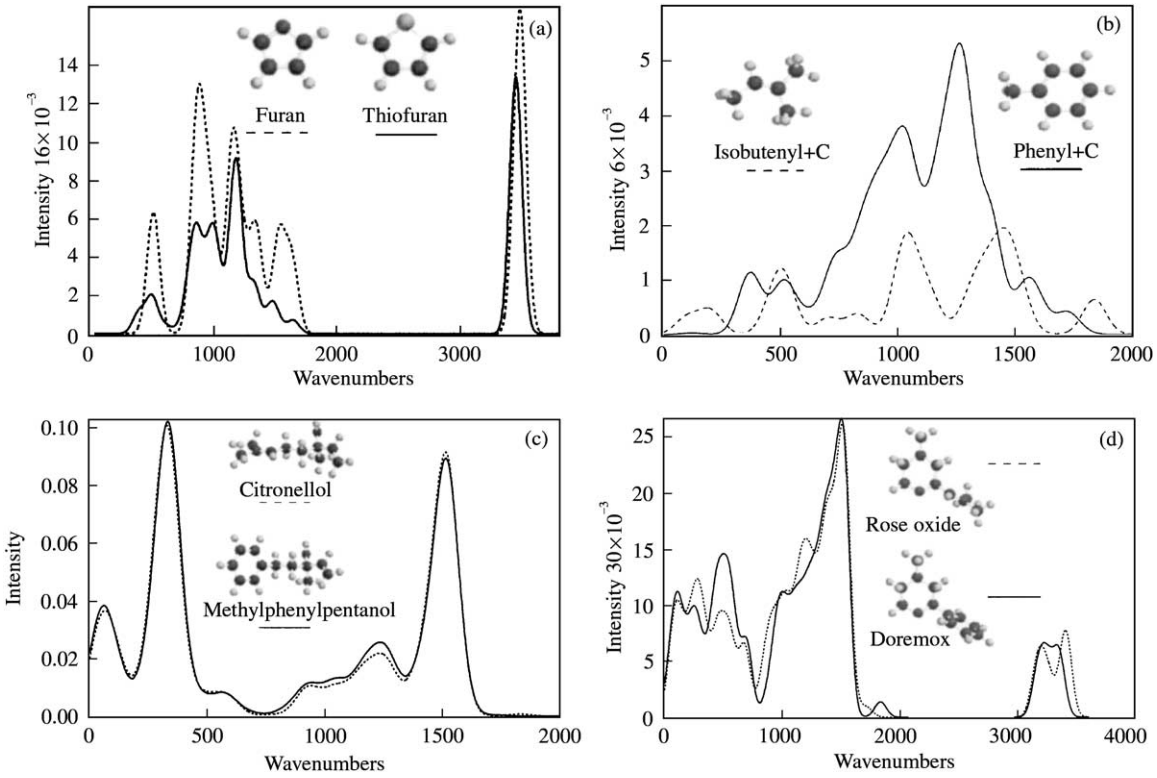

FIG. 7. Structures and spectra of (a) furan and thiofuran. The structures are rather similar, but odor character and spectra are quite different. (b) The isobutenyl and phenyl fragments, with one extra carbon added to represent attachment point to a hypothetical molecule. Shapes and spectra are very different. (c) citronellol and methylphenylpentanol and (d) rose oxide and doremox, two example cases where the isobutenyl–phenyl replacement is without much effect on both spectra and odor character.

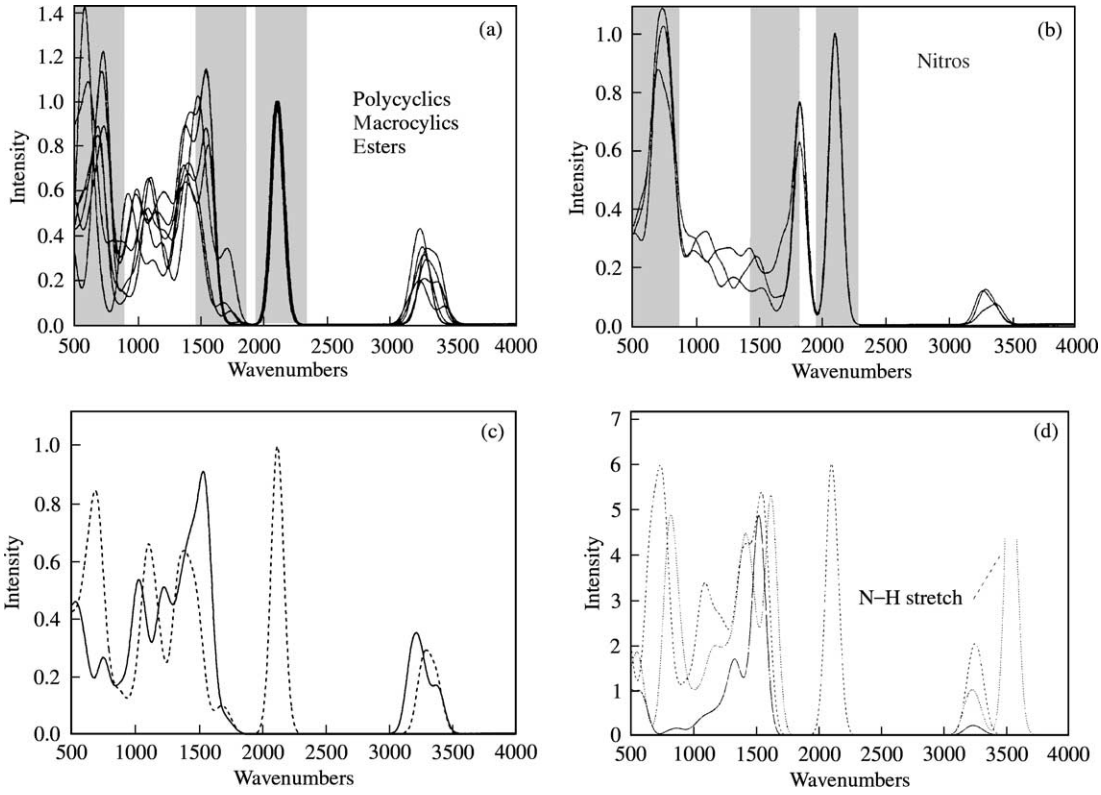

FIG. 8. Structures and spectra of (a) three polycyclic musks (tetralin, indane and hydroxycoumarin), three macrocyclin musks (muscone, MuskR1 and exaltolide), and two ester musks (cyclomusk and helvetolide). Peaks within the three 400 wavenumber-wide receptor bands (light gray) are postulated to be responsible for the musk odor of these odorants. (b) The same bands, depicted with the spectra of three nitro musks (musk ambrette, musk ketone and moskene). The spectra give a similar pattern of fit to the three bands. (c) A musk that does not fit this pattern: isochroman (——) lacks the 700 wavenumber band. (d) A spectral explanation for the remarkable finding that the imine equivalent of a macrocyclic musk civetone (- - - -) hexadecamethyleneimine, (▪▪▪▪▪) still smells of musk, but that the corresponding alcohol (——), does not.

4.1.1. *Reporter Charges*

Macrocyclic musks provide an insight into some basic characteristics of IETS spectra which may be unfamiliar to readers used to IR line intensities governed by dipole strength. In "simplified" IETS as used here the direction of charge movement in a given mode has no bearing on line intensity. Collective modes of the whole molecule which in IR add up to a small dipole moment instead give rise to large intensities, particularly if they involve movement of a polar group. In a 16-carbon keto macrocyclic, for example, the largest charge ($\approx \pm 0.5$e) is borne by the constituent atoms of the keto group. Whenever a vibrational mode involves movement of the keto group, its intensity will be greatly increased.

Fig. 8(d) shows the normal spectrum of the 16-carbon macrocyclic. Replacement of the keto group with an imine group, which is known, suprisingly, to preserve a musk character (Ruzicka *et al.*, 1934), still yields a musk-like spectrum [Fig. 8(d) dotted trace]. C = O and NH groups act here as "reporter groups" for motions of the macrocycle. By contrast, the corresponding (non-musky) alcohol, in which the OH group is outside the ring, and thus differently coupled to ring motions, has a completely altered spectrum more akin to that of a woody odorant [Fig. 8(d) black trace]. Furthermore, whereas C = O and N–H have stretch modes well outside the "fingerprint" region 1000–1500 cm^{-1}, there is a very strong C–OH stretch mode around 1500 which gives rise to the main peak. Similarly, setting the charge on the keto group to zero in the 16-carbon musk destroys the musk pattern, greatly lowers overall intensity and once again gives a woody pattern.

4.1.2. *Macrocyclic Ring Length and the Musk Odor Character*

The identification of three vibrational bands as defining musk odor can be applied to the baffling structure–odor relation between ring length and musk character in musk ketones, first described by Dyson in 1929 (see Mookherjee & Wilson, 1982). When cyclic ketones of increasing ring length are synthesized, it is found that only rings with 14 and 15 carbons (C14 and C15) have a musk odor. C6–C8 smell minty, C9–C12 camphoraceous, C13 woody, C16–C19 smell of civet (getting fainter as C number increases) and C20 is odorless. Considering the flexibility of these molecules, it is very hard to understand what structural feature could be exhibited only by C14 and C15 but not by their immediate neighbors.

A vibrational approach gives a different picture. Band 3 (C = O stretch) is of almost constant intensity as carbon number increases. The pattern, if any, must therefore be in bands 1 and 2. Figure 9(a) shows the spectra in the 500–2000 wavenumber region for C6–C20 rings, with the C14 and C15 spectra highlightened in bold. Intensity in both bands 1 and 2 is highest for these two odorants. Fig. 9(b) plots integrated intensity in bands 1 + 2 [gray regions in Fig. 9(a)] vs. number of carbons. C14 and 15 (filled circles) are outlier points in the series, suggesting that the specificity of C14 and C15 lies in their vibrations, not their shape. This is not an artifact of MNDO calculations, C14 and C15 spectra are also extremal in these two bands when using AM1 and PM3 parameters.

4.1.3. *Case Study 1: Calculating a Linear Musk*

There is considerable interest in devising new musks that are neither macrocyclic nor polycyclic. Macrocyclic musks (Williams, 1999) tend to be relatively expensive because of adverse thermodynamic factors in the synthesis, whereas polycyclics tend to persist in the environment. It seemed interesting to approach the problem of creating new musks using the algorithm to calculate IETS spectra. The problem cannot be solved directly, because it is as yet impossible to go from spectrum to structure. However, the method described here readily lends itself to the narrowing down of a range of structures and selection of those with the most promising spectra.

A linear musk molecule would be desirable, because it may be easier to make and to break down. Comparison of the spectra of civetone and its open-ring congener 8-ketohexadecane [Fig. 10(a)] shows them to be very similar. This is consistent with the view that ring closure will affect modes only at very low energies, likely well below 100 cm^{-1}. It also tallies with the existence of the remarkable linear musk ethyl citronellyl oxalate. Yoshii *et al.* (1994) have shown that its minimum energy configuration is folded over to

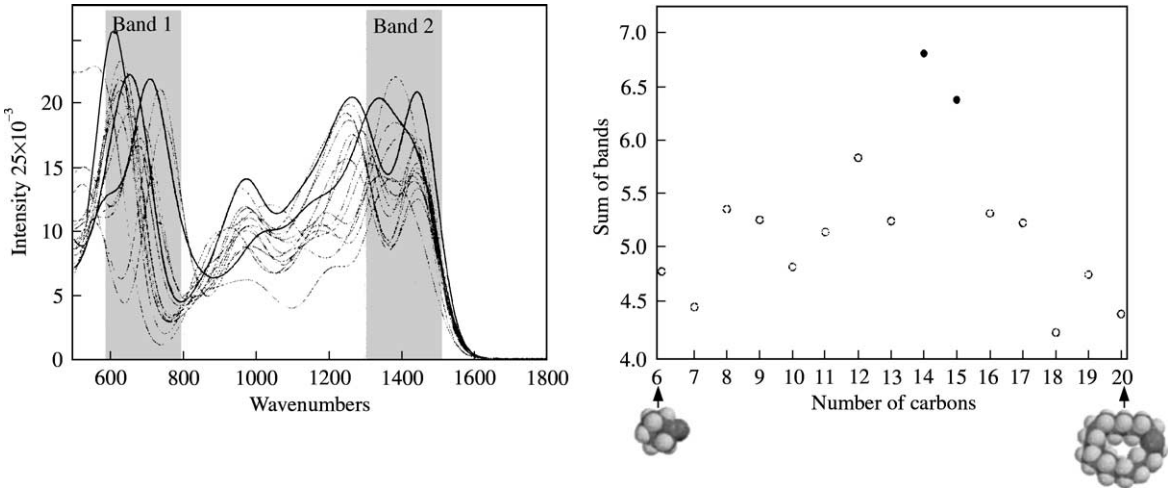

FIG. 9. (a) The spectra of cyclic ketones with 6–20 carbons. C14 and C15, the only ones with musk character, are black, the rest gray (b) integrated intensity in bands 1 + 2, for C6–20. See Section 4.1.2.

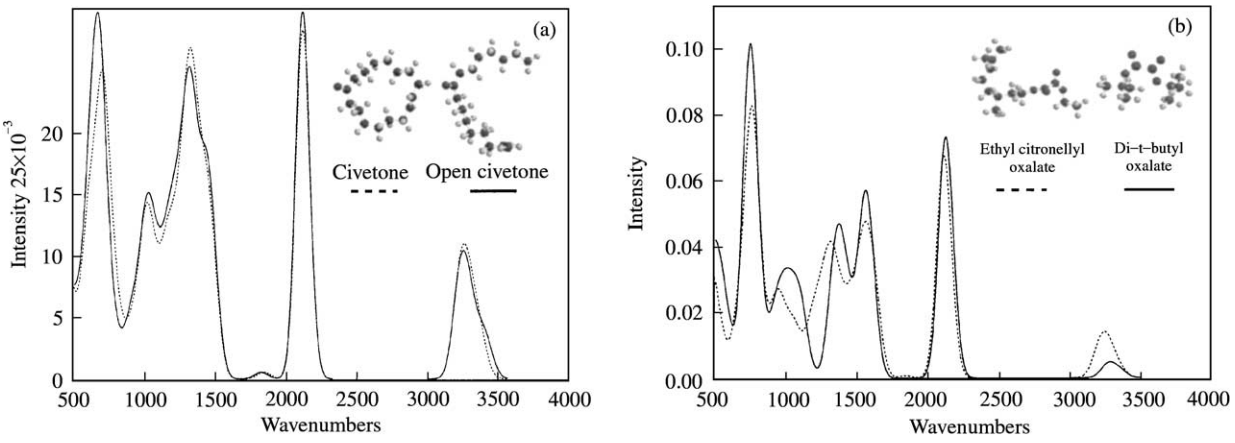

FIG. 10. (a) Structure and spectra of civetone and its open ring congener. Though ring closure is essential to the musk odor (open ring derivatives tend to be odorless), it has little effect on the spectrum, suggesting that fit into the receptor site is responsible for the lack of odor (see Section 3.2.1). (b) The linear musk ethyl citronellyl oxalate and the novel "musk" di-*t*-butyl oxalate, whose odor was predicted from spectral calculations.

resemble the conformation of a macrocyclic musk [Fig. 10(b)]. This suggests that the requirement for cycle closure in macrocyclic musks is purely steric, to enable the molecule to fit in the receptors.

Inspection of the vibrational spectrum of ethyl citronellyl oxalate reveals that the peak around $740\,cm^{-1}$ is due to a scissor mode of the two adjacent carbonyls in the oxalate moiety. The "target" then becomes a smaller, more compact oxalate still possessing the correct vibrations. Calculation of the symmetric alkyl ester derivative diethyloxalate showed that the $750\,cm^{-1}$ peak was still present, but that the other peaks were rather different. Recalling that many musks contain bulky dimethyl and *t*-butyl groups, it seemed natural to calculate the di-*t*-butyl oxalate. Its spectrum is shown in Fig. 10(b). A closer approximation to the ethyl citronellyl oxalate is achieved. Di-*t*-butyl oxalate has the advantage of being commercially available, and its odor can be checked. Remarkably, it has a fruity–musky odor character resembling that of ambrettolide. It is, however, rather weak. This is probably due to the presence of four oxygen atoms in an otherwise small molecule, which lowers its partition coefficient $\log P$. No doubt-related structures, less polar in character, could be found, possibly related to the strong odorant diacetyl, i.e. lacking the two ester oxygens. Among these a strong linear musk will probably be found.

4.2. AMBER

The amber character is distinctive, fresh and pungent, and reminiscent of isopropanol. Ambers are remarkably diverse in chemical structure. The spectra of seven ambers (karanal, amberketal, spirambrene, cedramber, ambrox, okoumal and ysamber) are shown in Fig. 11(a). They resemble those of musks save for the absence of the peak at 700, and differ from non-ketonic woods (below) in the presence of a pronounced shoulder made of two peaks, one around $1000\,cm^{-1}$, the second near $1300\,cm^{-1}$, below the main peak. In some ambers like cedramber, spirambrene (very similar in smell) and ysambrene, this shoulder is large enough to compete with the main peak. It is not clear whether the size of the $1300\,cm^{-1}$ peak correlates with odor character. The spectra of isopropanol and propanol are also shown for comparison [Fig. 11(a) inset]: isopropanol has the peak at $1300\,cm^{-1}$, whereas propanol, whose smell character is completely different, like that of ethanol has a trough in the corresponding position. The difference is due to a single antisymmetric C–C stretch mode centered on the middle carbon of isopropanol, and involving OH bend as well, hence its large intensity.

4.3. WOODS

The woods present an interesting puzzle. Woody is a broad odor category which ranges

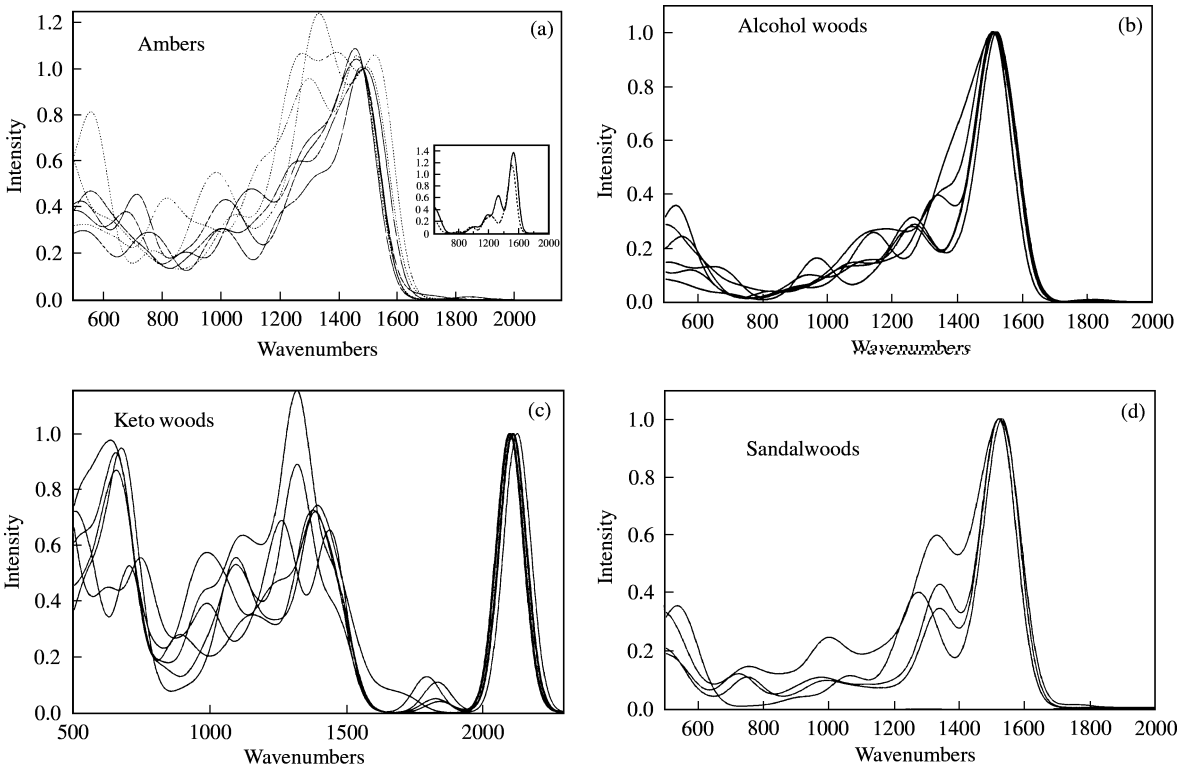

FIG. 11. (a) The spectra of seven structurally unrelated ambers (karanal, ambrox, amberketal, spirambrene, cedramber, okoumal and ysamber). The 1500 wavenumber peak is strongly asymmetric and slopes almost linearly to the left in four of them (red traces). In the three dotted traces (spirambrene, cedramber and ysamber), the secondary peaks below 1500 are sufficiently large to exceed the 1500 peak. For ease of comparison, all traces have been normalized on 1484 wavenumbers. The inset shows the spectra of isopropanol (reminiscent of ambers) and propanol (ethanol-like smell). Only isopropanol (red trace) has the peak below 1400. (- - - -) isopropanol; (——) propanol (b) The spectra of six structurally different woody alcohols: cedrol, kohinool, guaiol, vetivenol, camekol and limbanol. The 1500 wavenumber peak is more symmetrical, the shoulder at $\approx$1300 less prominent. The rise below 800 wavenumbers is not seen in smaller, non-woody alcohols such as octanol, but otherwise the spectra are quite similar. Spectra normalized on the 1500 peak for comparison. (c) The spectra of six "keto" woods (cedrenone, polywood, suberanone, iso-E super, spiroketone and vertofix). The spectra are different from each other and from woody alcohols. (d) The normalized spectra of four structurally unrelated sandalwoods (beta-santalol, osyrol, androstenol and bucyclodecanol). As expected, the spectra are rather similar to woods, but the shoulder below 1500 is broader and more pronounced.

from camphoraceous woods like cedrol to earthy smells like patchouli and vetiver. The reference set of woody smells chosen is shown in Fig. 1 (W1–W12). They are the alcohols cedrol, guaiol, vetivenol, kohinool, limbanol and camekol, and the ketones cedrenone, vertofix, spiroketone, suberanone, isoE, polywood. The spectra of the alcohols [Fig. 11(b)] are remarkably similar, with a large peak around 1500 cm^{-1}, a small shoulder at 1250 and a trough around 750. Note the remarkable structural diversity of these chemically unrelated molecules: guaiol is a bicyclic $7+5$ skeleton, kohinool is a highly methylated heptanol, cedrol is a tricyclic sesquiterpene, limbanol a substituted cyclohexene, and camekol a norbornane derivative.

By contrast, the spectra of the keto woods are rather different from each other and from wood alcohols, and more reminiscent of musks [Fig. 11(c)], but with the peaks at 700 and 1500 cm^{-1} seemingly shifted to lower wavenumbers. It is not yet clear whether this ambiguity between keto woods and musks is a calculation error or the reflection of the woody territory in odor space extending very close to that of musks. It is also unclear whether the fact that two different families of spectra pertaining to the wood character reflects an improper naming.

There is an additional problem associated with the wood alcohols, namely that their spectra are quite close to those of low molecular weight aliphatic alcohols with smells that cannot be

described as woody, like octanol. The main difference appears to be that between 500 and 600 cm^{-1}, the intensity of larger (woody) alcohols is higher because of a larger number of low-frequency modes. It is not clear whether this is sufficient to account for the difference in odor character.

4.4. SANDALWOODS

Sandalwoods have been studied extensively because of their great commercial importance, and their structure–odor relations are of great interest, because of the striking diversity of structures possessing a sandalwood odor. Figure 2 shows four sandalwoods (SW1–SW4) taken from Rossiter (1996) with very diverse structures. They are androstenol, santalol, bicyclododecanol and osyrol. The latter is of particular interest, because despite its fine sandalwood character, it breaks all the structural rules of sandalwoods (Brunke, 1981). The spectra of these sandalwoods [Fig. 11(d)] are remarkably similar, positioned between woods and ambers in that the 1300 cm^{-1} shoulder is present, though smaller than in the ambers, and the 1000 cm^{-1} peak is absent.

For a closer comparison between ambers, woods and sandalwoods, it is interesting to plot the "fingerprint" (1000–1500 cm^{-1}) region of their spectra normalized to the height of the CH stretch peak [Fig. 12(a)]. It is clear that the three categories (at least in this sample) can be differentiated by the amplitude of their peaks, as well as the shape. It is also possible to average the spectra in each category [Fig. 12(b)]; the pattern shown above then becomes clearer, with sandalwoods and woods rather close but distinct and ambers markedly different.

4.5. CASE STUDY 2: THE ODOR OF VIOLETS

Kraft (1999) has published a detailed study of violet odorants, both classical and novel. Violet and iris odorants have complex woody–fruity–floral profiles, and rather different structures. I have chosen 18 of the most significant structures from his study, labelled V1–V18 and illustrated in Fig. 13. V1–V8 are classical violet odorants.

Kraft states: "Interestingly, the constitutional irone-isomer (V5) with seven-membered ring was said to be reminiscent of 8-methylionone (V4) with a pronounced floral character. While the constitutional ionone-isomer V6 is more reminiscent of irone (V3) with an additional fruity respberry note. Two *seco* ionones, respectively, 5 - tert - butyl - 6 - methylhepta - 3,5 - dien - 2 - one (V7) and Koavone (V8), are known to possess the odor characteristics of ionone (1/2) and B-methylionone (4), respectively." In other words, V5 = V4, V6 = V3, V7 = V1,2 and V8 = V4. Fig. 14(a–d) tests for similarities in the spectra

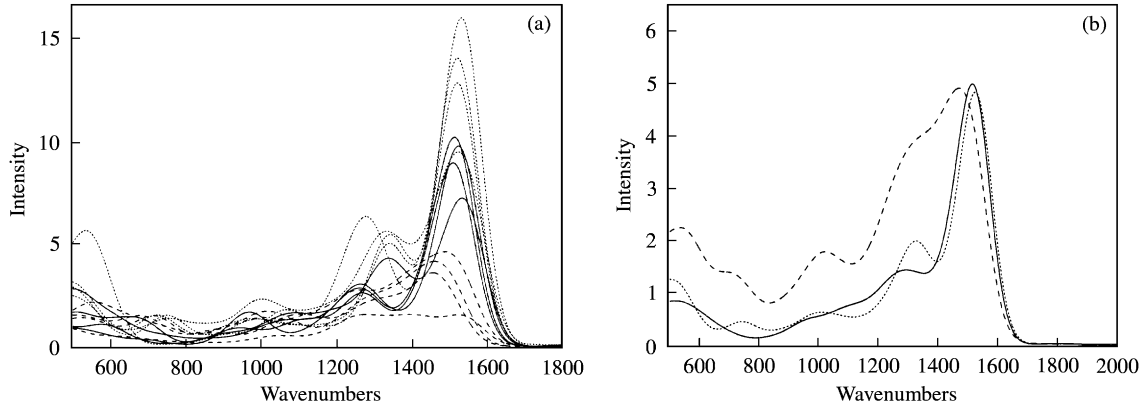

FIG. 12. (a) A comparison of the ambers, woods and sandalwoods in Fig. 10, normalized to the height of the CH stretch peak (not shown). A clear pattern of amplitudes is visible, with the sandalwoods largest, the woods intermediate and the ambers smallest. In addition, it is clear that in this set of odorants the peak of the sandalwoods around 1300 corresponds approximately to a trough in the woods, and that the 1500 peak in the ambers is shifted to lower wavenumbers by 50–100. (- - - -) Ambers; (——) Woods; (-·-·-) Sandalwoods, (b) comparison between averaged ambers, woods and sandalwoods. The traces are first normalized to the height of the 1500 peak, then added and averaged. The features seen in Fig. 10 and 11(a) are clearly visible: the difference between woods and sandalwoods around 1300, and the shift in the 1500 peak in the ambers (- - - -) Ambers; (——) Woods; (-·-·-) Sandalwoods.

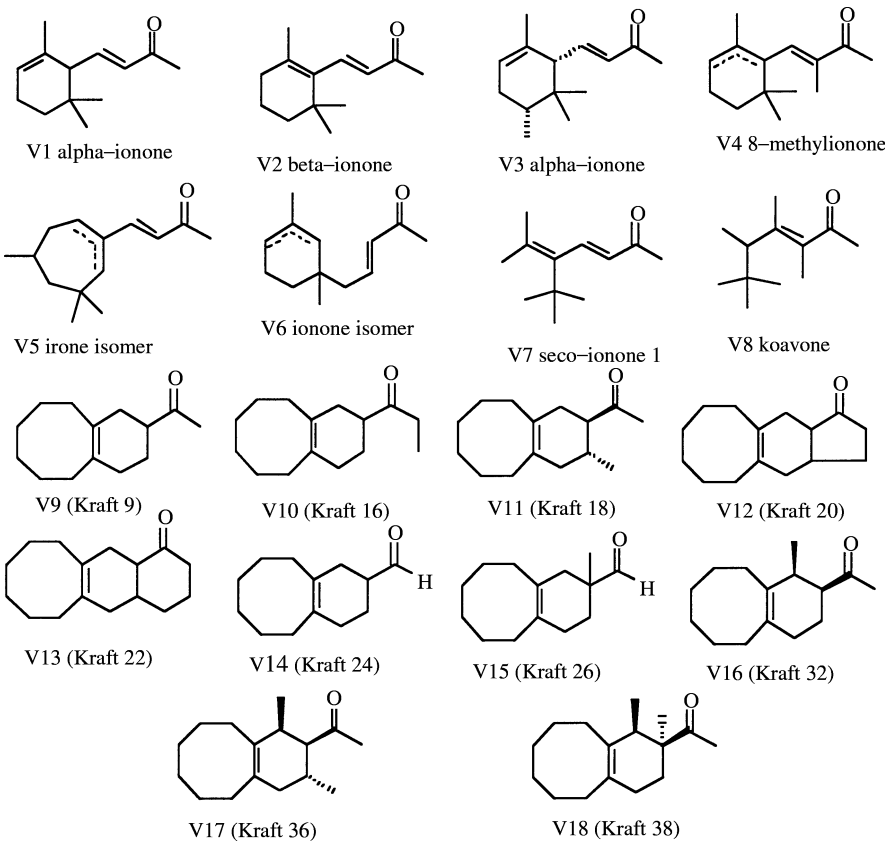

FIG. 13. The violet odorants discussed in Kraft (1999). Numbers in parentheses refer to Kraft's original numbering. V1-8 are classic violet odorants, V9-18 are novel syntheses.

for these odor relationships. Though the V1–8 spectra are different from each other, in every case the similarities on odor are reflected in close similarity in spectra. Particularly remarkable are V6–V3 and V8–V4, where spectra match very well while the structures are quite different. The algorithm also correctly predicts the fact that compounds V12–V15 do not smell like V2, and the V-16 is close while V18 is completely different. It also predicts the reported closeness of V9–V2. However, it fails to predict the fact that V10 is closer to V2 than V11 (not shown).

4.5.1. *Quantitative Comparison of Violet Spectra*

When dealing with closely related spectra as in the previous section, it is useful to put spectrum comparison on a quantitative basis. Various methods can achieve this. The one chosen here has the merit of simplicity. If two spectra are to be compared, the ratio of the two spectra at each wavenumber (smaller value/larger value) r is calculated. The ratios are integrated over a chosen interval of wavenumbers, and normalized by dividing by the number of points integrated. To account for relative odor constancy over a large range of concentrations, one assumes that only ratios between peaks matter to odor character, not absolute values. This allows the scaling of spectral amplitude, (not wavenumber) to find the optimal (largest) R before integration. If the spectra are identical, this number R will be equal to 1. This gives a crude and not very sensitive measure of spectral overlap: even completely unrelated spectra will tend to have $R = 0.3$–0.4. To give a greater range, a change of variable to $1/1\text{-}R$ is done.

Figure 15 illustrates the 18×18 matrix of optimal R values for violet odorants. Below the diagonal, the numerical values of R are given. Above the diagonal, the (symmetric) values are color-coded, with a threshold set at 3.5. The

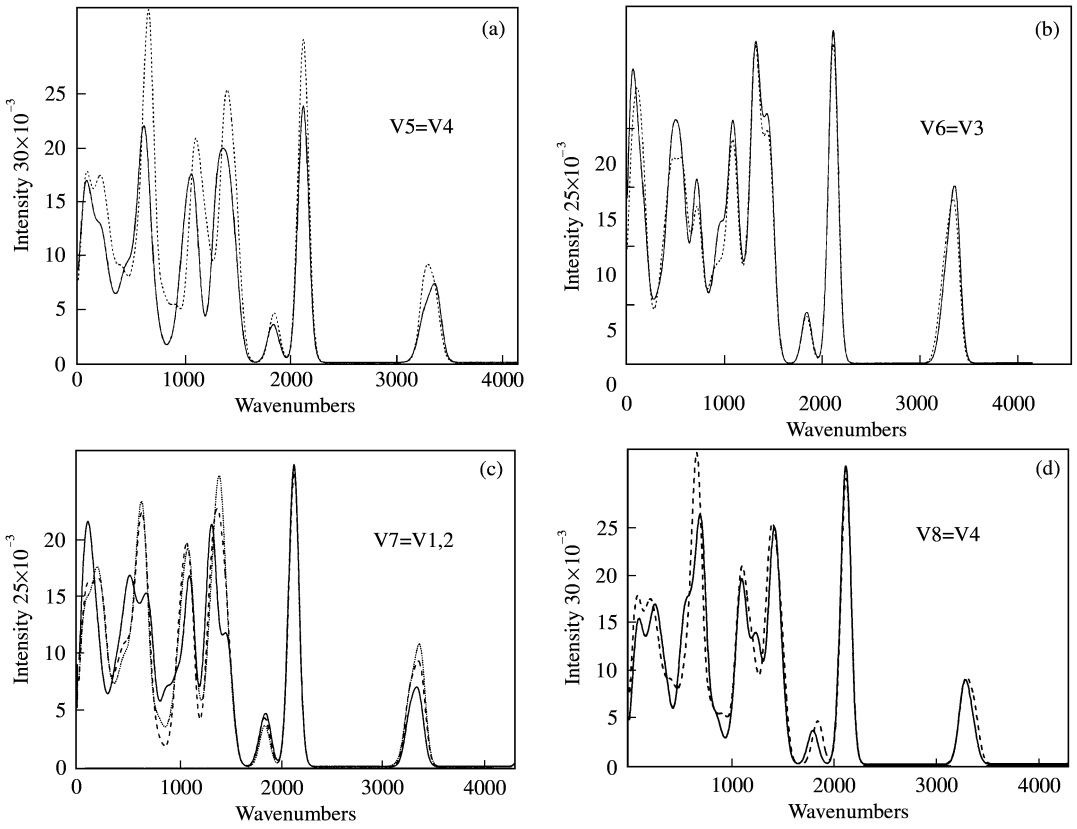

FIG. 14. The spectra of violet odorants whose odors are reported as similar by Kraft (1999). (a) Irone isomer and methylionone (b) ionone isomer and alpha-irone (c) seco-ionone, alpha ionone and beta ionone and (d) Koavone and methylionone.

black squares indicate a low similarity between spectra, and the colors from dark green through light green, yellow, orange and red indicate increasing values of R.

As expected, the matrix finds a high degree of similarity between the reference violet odorants V1–V8. In particular, it correctly predicts V6 = V3 (square labeled (1) and V8-V4 (2). However, it fails to predict the similarity between V5 and V4 (6) visible in the spectra [Fig. 14(a)]. The reason is that the spectra of V5 and V4, though very similar in shape, appear to be translated along the wavenumber axis, and therefore overlap less. Note in this context that while a complete overlap should guarantee similarity of odor, the converse is not true. If the sensing is done in bands, lack of spectral overlap with overall similarity in shape could nevertheless give a similar odor character. The best analogy for this comes from color vision. For example, two sets of three narrow band illuminants set in different positions, but giving the same amount of excitation of the three cones would give the same color sensation without *any* spectral overlap at all.

Interestingly, the matrix predicts other similarities in odor which were not central to the purpose of the violets study. For example, compounds V9, V11, V16 and V18 are all described as woody, and the R values reflect this (squares labelled 3–5). It also predicts a similarity between the aldehydes V14 and V15 of which the author makes no mention, and between V10 and V13, not described in the paper.

5. Towards on Odor Map

Another approach to quantitative spectral comparison involves simulating the sensing by bands. As has been emphasized in Section 2.3 their number, width and position is unknown. It is nevertheless instructive to see what the properties of an odor space analogous to

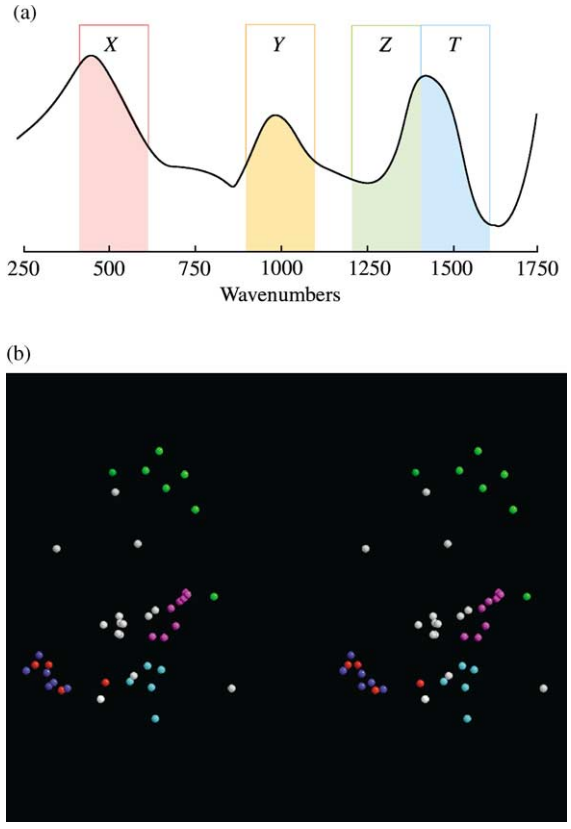

FIG. 16. The construction of a three-dimensional odor map based on the color vision chromaticity diagrams. (a) The spectrum is divided into bands 200 wavenumbers wide, and the intensity in each band is integrated to give four numbers. After normalization and ratioing, this yields a three-dimensional map. One such map is shown in (b), featuring 45 odorants from this study. Odor characters are color-coded: blue = woods, red = sandalwoods, light blue = ambers, green = bitter almonds, purple = violets and white = musks. The stereo diagram is intended for cross-eyed viewing.

doi: 10:1006 jtbi.2001.2504

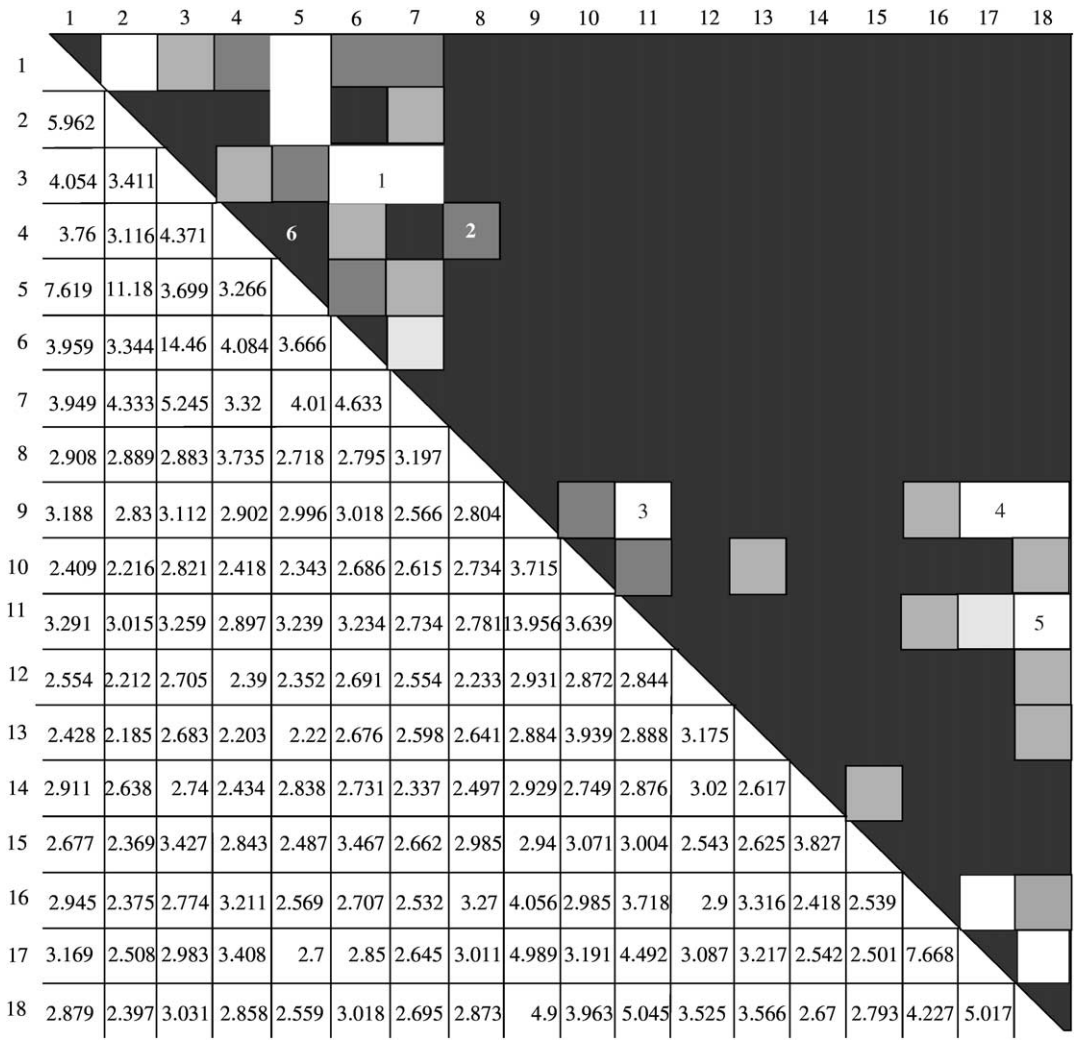

FIG. 15. Spectral comparison matrix for the 18 violet-related odorants shown in Fig. 13. The matrix is symmetric across the diagonal. The lower half shows overlap indices (see Section 4.5.1 of text for method of calculation), the upper half translates values into brightness for ease of comparison). Brightness from black to white indicates increasing values of index. Numbered squares are referred to in text.

color space would be (for a comprehensive review of color measurement, see Berger-Schunn, 1994). Humans are trichromats, which enables (after normalization, since ratios, not absolute values, determine color) the construction of the familiar two-dimensional color maps known as chromaticity diagrams. Discrimination of even the small subset of odorants described in this paper will clearly require more than three bands.

Figure 16(a) illustrates band position and normalization method for a four-band system. The spectral intensity within each band is integrated, bands X Y and Z are normalized by dividing by the total intensity in all bands $X+Y+Z+T$. The result is a three-dimensional map [stereo Fig. 16(b)] in which every point represents a single odorant. Colors indicate odor character, with blue = woods, red = sandalwoods, cyan = ambers, white = musks, green = bitter almonds and purple = violets. Inspection of the stereo diagram shows that different smell characters inhabit distinct territories. Sandalwoods and woods are close, as may be expected from their closely related spectra. An amber territory separates them from violets, which come close to an extended cloud of musks, while bitter almonds lie in a cluster some distance away. The position of these points depends strongly on band position, width and normalization method.

Normalization is less legitimate for odor than for color, because odor character varies more markedly than color with stimulus intensity. Figure 16(b) nevertheless clearly shows that a plausible analogue of a chromaticity diagram, which might be termed an "osmaticity diagram", can be built even using these crude assumptions. Filling out this color space and exploring its properties under a variety of different mappings is a matter for further investigation.

6. Conclusions

Despite its simplicity, the method for spectrum calculation described here is strikingly successful at predicting similarities and differences in odor character between odorants belonging to widely different structural and odor classes. The successes, insofar as they form too large a body of coincidences to be explained by chance alone, provide circumstantial support for a vibrational theory. Direct evidence for or against vibration theory can only come from biological experiments. In the meantime, this method is a small but clearly useful step towards rational odorant design. It seems to be the first general SOR theory to date possessing *predictive* power. The total cost of hardware and software used in these calculations amounts to $\$ < 5\,\mathrm{k}$. Given the cost of synthesis, if the method eliminates bad target molecules and suggests good ones in a synthesis program, it could pay for itself in a week's work.

The method nevertheless clearly fails in a number of instances. These failures are harder to interpret at present. They could be due to (a) a misreporting of an odor profile in the literature (b) a more complicated mapping of spectrum to odor, such that more than one spectral pattern maps onto a given odor territory or (c) imperfections in the algorithm. (a) is unlikely with the examples we have chosen, whereas (b) and (c) are to be expected, given that only a tiny subset of odorants has been explored, and the crudest of calculation methods has been used. Further work will address these questions.

At present the method is best suited to spectrum comparison between a "target" molecule and planned syntheses. Inspection of the spectra or a simple overlap criterion could determine which spectra are closest to the target. Future applications should aim at the more ambitious goal of identification of odor character from the spectrum directly. Before that can be done, the spectral calculation method has to be validated carefully, applied to a large number of odorants, and descriptors for spectral features put in correspondence with odor characters. Finally, an even more ambitious aim might be to solve what looks like a formidable inverse problem, i.e. design a molecule to fit a particular desired spectrum. Getting a clearer understanding, for example, of why isobutenyl and phenyl are interchangeable, or why sulfur seems good at replacing double bonds may point the way to a solution.

I thank Professor Peter Mobbs for his support and hospitality in the Physiology Department, and Tim Arnett Frank Hoffmann and an anonymous referee for suggesting many improvements to the paper.

REFERENCES

Arctander, S. (1994). *Perfume and Flavor Chemicals*. Carol Stream, IL: Allured Publishing.

Berger-Schunn, A. (1994). *Practical Color Measurement*. John Wiley: New York.

Boelens, H. (1974). Relationship between the chemical structure of compounds and their olfactive properties. *Cosmetics and Perfumery* **89,** 1–7.

Boelens, H. & Heydel, J. (1973). Chemische Konstitution und Geruch. *Chem. Zeitung* **97,** 1–8.

Brunke, E. J. (1981). Dragoco Report 251.

Dyson, G. M. (1938). The scientific basis of odour. *Chem. Ind.* **57**, 647–651.

Frater, G., Bajgrowicz, J. A. & Kraft, P. (1998). Fragrance chemistry. Tetrahedron **54,** 7633–7703.

Hehre, W. J., Yu, J., Klunzinger, P. E. & Lou, L. (1998). A brief guide to molecular mechanics and quantum chemical calculations. Wavefunction, Inc Irvine, CA, U.S.A.

Kraft, P. (1999). Design and synthesis of violet odorants with bicyclo [6.4.0] dodecene and bicyclo [5.4.0] undecene skeletons. *Synthesis* **4**, 695–703.

Kraft, P., Eichenberger, W. & Fráter, G. (1999). Synthesis of a constitutional isomer of nerol by consecutive Ireland-Claisen and Cope rearrangements. *Eur. J. Org. Chem.* 1999, 2781–3010.

Kraft, P., Bajgrowicz, J. A. & Fráter, G. (2000). Odds and trends: recent developments in the chemistry of odorants. *Angew. Chem. Int. Ed. Engl.* **39,** 2980–3010.

Malnic, B., Hirono, J., Sato, T. & Buck, L. B. (1999). Combinatorial receptor codes for odors. *Cell* **96,** 713–723.

Moncrieff, R. W. (1949). The Chemistry of Perfumery Materials. London: United Trade Press.

MOOKHERJEE, B. D. & WILSON, R. A. (1982). Musks. In: *Fragrance Chemistry* (Theimer, E.T., ed.), New York: Academic Press.
MORI, K. & SHEPHERD, G. M. (1994). Emerging principles of molecular signal processing by mitral/tufted cells in the olfactory bulb. *Semin. Cell Biol.* **5,** 65–74.
OHLOFF, G. (1994). Scent and Fragrances: the Fascination of Odors and their Chemical Perspectives. Berlin: Springer.
ROSSITER, K. J. (1996). Structure–odor relationships. *Chem. Rev.* **96,** 3201–3240.
RUZICKA, L., SALOMON, G. & MEYER, K. E. (1934). *Helv. Chim. Acta* **17,** 882.
SELL, C. (1999). Chemoreception, In: (Pybus, D. H. & Sell, C., eds), *The Chemistry of Fragrances*, pp. 216–226. Cambridge, Royal Society of Chemistry Paperbacks.
SLEIGH, A. K., PHILLIPS, W. A., ADKINS, C. J. & TAYLOR, M. E. (1986). A quantitative analysis of the inelastic electron tunnelling spectrum of the formate ion. *J. Phys. C* **19,** 6645–6654.
STURM, W. (1978). Haarmann and Reimer Contact **21,** pp. 20–27.
TURIN, L. (1996). A spectroscopic mechanism for primary olfactory reception. *Chem. Senses* **21,** 773–791.
TURIN, L. & YOSHII, F. (2002). Structure–odor relations: a modern perspective. In: *Handbook of Olfaction and Gustation* (Doty, R., ed.). New York: Marcel Dekker.
WANNAGAT, U., DAMRATH, V., HUCH, V., VEITH, M. & HARDER, U. (1993). Sila-Riechstoffe und Riechstofffisostere XII. Geruchsvergleiche homologer organoelementverbindungen der vierten hauptgruppe (C, Si, Ge, Sn). *J. Organometallic Chem.* **443,** 153–165.
WILLIAMS, A.S. (1999). The synthesis of macrocyclic musks. *Synthesis* **10,** 1707–1723.
WRIGHT, R.H. (1977). Odor and molecular vibration: neural coding of olfactory information. *J. theor. Biol.* **64**, 473–502.
YOSHII, F., HIRONO, S, & MORIGUCHI, I. (1994). Relations between the odor of (R) ethyl citronellyl oxalate and its stable conformations. *Quantitative Structure-activity Relationships* **13**, 144–147.
ZAKARYA, D., YAHIAOUI, M. & FKIIHTETOUANI, S. (1993). Structure–odor relations for bitter almond odorants. *J. Phys. Org. Chem.* **6,** 627–633.

APPENDIX

Partial charges, vibrational mode frequencies and calculated IETS intensities for trans-2-hexenal

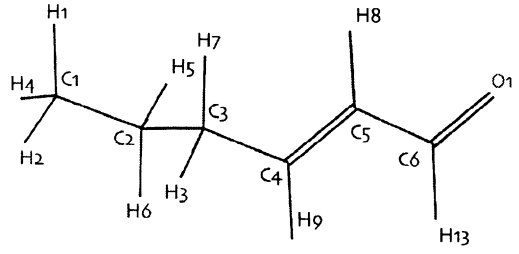

Partial charges	
H_1	−0.015716
C_1	0.049337
H_2	−0.013774
C_2	−0.045803
C_3	0.140986
H_3	−0.025380
H_7	−0.014811
C_4	−0.014103
C_5	−0.298855
H_8	0.100306
C_6	0.680691
O_1	−0.499926
H_{13}	−0.078995
H_9	0.029047
H_5	0.008417
H_6	0.004039
H_4	−0.005459

cm^{-1}	Intensity
64.84	0.00619
84.61	0.00641
104.99	0.00691
174.31	0.01093
207.14	0.00061
243.48	0.00722
335.30	0.00348
373.80	0.00608
537.41	0.00998
583.81	0.01121
800.49	0.00054
898.24	0.00777
954.62	0.00248
990.37	0.00211
1021.60	0.00128
1073.77	0.01589
1104.28	0.00271
1190.72	0.00045
1206.43	0.00272
1234.13	0.00211
1236.51	0.00547
1242.85	0.00178
1274.37	0.00573
1344.62	0.00411
1371.02	0.00632
1387.66	0.00118
1437.93	0.00832
1442.06	0.00064
1445.60	0.00012
1448.91	0.00091
1452.93	0.00020
1478.82	0.00081
1492.89	0.00020
1827.54	0.00381
2113.35	0.02902
3210.74	0.00031
3228.37	0.00031
3244.91	0.00832
3261.76	0.00010
3268.86	0.00021
3277.35	0.00027
3289.19	0.00024
3342.72	0.00016
3357.36	0.00234
3380.63	0.00824